INTERNATIONAL JOURNAL FOR NUMERICAL METHODS IN FLUIDS
Int. J. Numer. Meth. Fluids 2005; **48**:501–519
Published online 23 February 2005 in Wiley InterScience (www.interscience.wiley.com). DOI: 10.1002/fld.936

Comparison of the GMRES and ORTHOMIN for the black oil model in porous media

Wenjun Li[1,‡], Zhangxin Chen[1,*,†], Richard E. Ewing[2,§], Guanren Huan[2,¶] and Baoyan Li[2,‖]

[1]*Department of Mathematics, Box 750156, Southern Methodist University, Dallas, TX 75275-0156, U.S.A.*
[2]*Institute for Scientific Computation, Texas A&M University, College Station, TX 77843-3404, U.S.A.*

SUMMARY

This paper deals with the application of the GMRES algorithm to a three-dimensional, three-phase black oil model used in petroleum reservoir simulation. Comparisons between the GMRES and ORTHOMIN algorithms in terms of storage and total flops per restart step are given. Numerical results show that the GMRES is faster than the ORTHOMIN for large-scale simulation problems. The GMRES uses only as much as 63% of the CPU time of the ORTHOMIN for some of the problems tested. Copyright © 2005 John Wiley & Sons, Ltd.

KEY WORDS: petroleum reservoir simulation; GMRES; ORTHOMIN; ILU preconditioner; black oil model

1. INTRODUCTION

As petroleum reservoir simulation technology gets more advanced, there are now new requirements from reservoir engineering. These requirements include very fine grids for development of new oil/gas fields, management of old oil/gas fields, and shortening of history match processes and simulation time, for example. On one hand, the fine grids lead to the size of a large-scale simulation model in terms of millions of unknowns. On the other hand, the shortening of history match and simulation time requires fast and accurate algorithms for solving large-scale systems. Furthermore, the systems of algebraic equations arising from the numerical discretization of the governing equations for multiphase flow in reservoirs have special

*Correspondence to: Zhangxin (John) Chen, Department of Mathematics, Box 750156, Southern Methodist University, Dallas, TX 75275-0156, U.S.A.
†E-mail: zchen@mail.smu.edu
‡E-mail: wli@mail.smu.edu
§E-mail: ewing@isc.tamu.edu
¶E-mail: huan@mail.smu.edu
‖E-mail: bli@mail.smu.edu

Received 23 June 2003
Revised 1 September 2004
Accepted 1 October 2004

properties. The coefficient (stiffness) matrices of these systems are sparse but non-symmetric and indefinite, for example. While sparse, their band structure is usually spoiled by wells that perforate into many gridblocks and/or by irregular gridblock structure. What is more, for petroleum simulation problems with a number of gridblocks of order 100 000, about 80–90% of the total simulation time is spent on solution of linear systems. Thus the choice of a linear solver is crucial to numerical simulation of multiphase flow.

The ORTHOMIN (orthogonal minimum residual) algorithm [1] has been applied to petroleum reservoir simulation and is still widely used in this area due to its ability to solve efficiently sparse, nonsymmetric systems of algebraic equations. However, it is well known that the GMRES (generalized minimum residual) [2] algorithm is more efficient and robust, particularly for solution of large systems. While this algorithm has been applied to numerical solution of the Navier–Stokes equations of compressible flow [3], it has not been employed in realistic petroleum reservoir simulations; especially, there is a lack of comparisons between these two algorithms for realistic simulations, as far as the authors know. The purpose of this paper is to apply the GMRES to numerical simulations using the black oil model in petroleum reservoirs. In particular, we compare it with the ORTHOMIN in terms of storage, total flops per restart, and CPU time for benchmark problems of the comparative solution projects (CSP) organized by the society of petroleum engineers (SPE) and for real oil field problems. Our numerical results show that the GMRES is faster than the ORTHOMIN for large-scale simulation problems. For some of the problems tested, the GMRES uses only as much as 63% of the CPU time of the ORTHOMIN.

The rest of the paper is organized as follows. For the purpose of comparison, in the next section, we review the ORTHOMIN and GMRES. Then, in Section 3, we compare these two algorithms in terms of their storage and flops. In Section 4, we state the black oil model we are simulating. In Section 5, we briefly mention the application of the GMRES to our black oil simulator. In Section 6, we apply the ORTHOMIN and GMRES to five simulation problems and compare them numerically. Finally, we make concluding remarks and mention future research in the last section.

2. THE ORTHOMIN AND GMRES ALGORITHMS

The ORTHOMIN is a truncated version of the GCR (generalized conjugate residual) algorithm and an efficient iterative solver for petroleum reservoir simulation [1]. For the purpose of comparison, a general ORTHOMIN(K) is briefly reviewed in Algorithm 1 for solution of a left preconditioned system

$$M^{-1}Ax = M^{-1}b \tag{1}$$

In Algorithm 1, for the purpose of illustration, $M = LU$ is an ILU factorization of A. A left-preconditioned GMRES is described in Algorithm 2, where $\hat{H}_m$ is upper Hessenberg from the Gram–Schmidt process. A variant of the GMRES, the FGMRES (flexible GMRES) [4], uses a different preconditioner at each step of the Arnoldi process. The Arnoldi process simply constructs an orthogonal basis for the preconditioned Krylov subspace

$$\kappa_m = \text{span}\{r_0, M_1^{-1}Ar_0, \ldots, (M_1^{-1}A)\cdots(M_{m-1}^{-1}A)r_0\}$$

Algorithm 1.

ORTHOMIN(K)

1. $M = LU$, where LU is an ILU factorization of A
2. **Start:** Set $r = b$, $x = p_0 = 0$, $Iter = 0$, and the values of ε, ITMAX, K
3. **Iteration:**
   (a) For $k = 1, K$ do
      i. Iter = Iter + 1
      ii. $u_k = M^{-1} r_{k-1}$
      iii. $v_k = A u_k$
      iv. $p_k = u_k$
      v. $q_k = v_k$
      vi. For $1 \leqslant j < k$, do
$$\begin{cases} \alpha_{jk} = (q_j, v_k)/(q_j, q_j) \\ p_k = p_k - \alpha_{jk} p_j \\ q_k = q_k - \alpha_{jk} q_j \end{cases}$$
      vii. $\beta_k = (q_k, r_{k-1})/(q_k, q_k)$
      viii. $x_k = x_{k-1} + \beta_k p_k$
      ix. $r_k = r_{k-1} - \beta_k q_k$
      x. Compute $\|r_k\|_2$, $RMX = \|r_k\|_2 / \|b\|_2$
      xi. If ($RMX \leqslant \varepsilon$ or Iter $\geqslant$ ITMAX), go to 4.
   (b) End do
   (c) $r_0 = r_K$
   (d) $x_0 = x_K$
   (e) Go to (a)
4. **End iteration**

The difference between the GMRES and FGMRES is that for the GMRES, all the $M_i = M$ are the same, and $z_i = M^{-1} v_i$ need not be stored for right preconditioners during computations. The FGMRES is more flexible and suitable to solution of difficult problems with complex preconditioners.

3. COMPARISONS

We assume that the same preconditioner M is used for both algorithms. Let STP and STA be the amount of storage for M and A, and let $FLOPP$ and $FLOPA$ be the total flops of computing $M^{-1}x$ and Ax, respectively, where x is a vector. Below we compare the ORTHOMIN and GMRES in terms of the storage and total flops per restart. The definition of a flop follows Reference [5]; i.e. a flop involves the operation $s + a * b$.

Algorithm 2.

Left preconditioned GMRES(m)

1. $M = LU$, where LU is an ILU factorization of A
2. **Start:** Choose an initial guess x_0 and the dimension of the Krylov subspace m. Set up a $(m+1) \times m$ matrix $\hat{H}_m$ with zero entries.
3. **Arnoldi process:**
   (a) Compute $r_0 = M^{-1}(b - Ax_0)$, $\beta = \|r_0\|_2$, and $v_1 = r_0/\beta$
   (b) For $j = 1, \ldots, m$, do
   - Compute $w_j = M^{-1}Av_j$
   - For $i = 1, \ldots, j$, $\begin{cases} h_{ij} = (w_j, v_i) \\ w_j = w_j - h_{ij}v_i \end{cases}$
   - Compute $h_{j+1,j} = \|w_j\|_2$ and $v_{j+1} = w_j/\|w_j\|_2$

   (c) Define $Z_m = [v_1, \ldots, v_m]$.
4. **Update:** $x_m = x_0 + Z_m y_m$, where
$$y_m = \text{argmin}\|\beta e_1 - \hat{H}_m y\|_2$$
5. **Restart:** If convergent, stop; else, $x_0 = x_m$ and go to 3

3.1. Comparison in terms of storage

Let NEQ be the number of partial differential equations (e.g. $NEQ = 3$ for the black oil model), NCV be the number of grids in the simulation domain, and $NRSTRT$ be the number of restarts, i.e. the number of vectors in the Krylov subspace.

For the ORTHOMIN, its main storage is as follows:

- Coefficient matrix: STA
- Preconditioner matrix: STP
- Krylov vector space: $2 * NEQ * NCV * NRSTRT$
- Other vectors such as RHS, RES, RA, RR: $4 * NEQ * NCV$
- Total storage: $STA + STP + 2 * NEQ * NCV * NRSTRT + 4 * NEQ * NCV$

For the GMRES, its main storage is given below:

- Coefficient matrix: STA
- Preconditioner matrix: STP
- Krylov vector space: $NEQ * NCV * NRSTRT$
- Vector space $Z_{NRSTRT} = [z_1, \ldots, z_{NRSTRT}]$: $NEQ * NCV * NRSTRT$

- Other vectors such as RHS, RES: $2NEQ * NCV$
- Matrix $\hat{H}_m$: $(NRSTRT + 1) * (NRSTRT + 6) + 3 * NRSTRT + 2$
- Total storage: $STA + STP + 2 * NEQ * NCV * NRSTRT + 2 * NEQ * NCV + (NRSTRT + 1) * (NRSTRT + 6) + 3 * NRSTRT + 2$

From these two counts, we see that when $NCV * NEQ > (NRSTRT + 5)^2/2$, the amount of storage of the ORTHOMIN is bigger than that of the GMRES.

3.2. Comparison in terms of total flops

For convenience, we consider the total flops of both algorithms per restart step.

For the ORTHOMIN, its main computational flops are

- Coefficient matrix: $FLOPA * NRSTRT$
- Preconditioner matrix: $FLOPP * NRSTRT$
- Inner product: $\{NRSTRT/2 + 2 * (NRSTRT + 1) * NRSTRT/2 + 2 * NRSTRT\} * (NEQ * NCV/2) = (NRSTRT/2 + 7/4) * NEQ * NCV * NRSTRT$
- Vector update: $\{4 + (NRSTRT + 1)\} * NEQ * NCV * NRSTRT = (NRSTRT + 5) * NEQ * NCV * NRSTRT$
- Total flop count: $\{FLOPA + FLOPP + ((NRSTRT/2 + 7/4) + 4 + (NRSTRT + 1)) * NEQ * NCV\} * NRSTRT = \{FLOPA + FLOPP + (NRSTRT * 3/2 + 27/4) * NEQ * NCV\} * NRSTRT$

For the GMRES, its main computational flops are:

- Coefficient matrix: $FLOPA * NRSTRT$
- Preconditioner matrix: $FLOPP * NRSTRT$
- Inner product: $\{(NRSTRT + 1) * NRSTRT/2 + NRSTRT\} * (NEQ * NCV/2) = (NRSTRT/4 + 3/4) * NEQ * NCV * NRSTRT$
- Vector update: $\{(NRSTRT + 1)/2 + 1 + 1\} * NEQ * NCV * NRSTRT = (NRSTRT/2 + 5/2) * NEQ * NCV * NRSTRT$
- Solving $y_m = \text{argmin} \|\beta e_1 - \hat{H}_m y\|_2$: $(NRSTRT + 1) * NRSTRT/2$
- Total flop count: $\{FLOPA + FLOPP + ((NRSTRT/4 + 3/4) + (NRSTRT/2 + 5/2)) * NEQ * NCV\} * NRSTRT + (NRSTRT + 1) * NRSTRT/2 = \{FLOPA + FLOPP + (NRSTRT * 3/4 + 13/4) * NEQ * NCV\} * NRSTRT + (NRSTRT + 1) * NRSTRT/2$

From these total flop counts, we see that when $NCV > NRSTRT$, in each restart step the total flops of the ORTHOMIN are bigger than those of the GMRES.

4. THE BLACK OIL MODEL

We briefly review the black oil model in a porous medium $\Omega \subset \Re^3$. In this model, it is assumed that no mass transfer occurs between the water phase and the other two phases (oil and gas). The black-oil model can handle a low-volatility oil system which consists of the gas (mainly methane and ethane) and oil components.

Let ϕ and K denote the porosity and permeability of the porous medium Ω, s_α, μ_α, p_α, u_α, B_α, and $K_{r\alpha}$ be the saturation, viscosity, pressure, volumetric velocity, formation volume factor, and relative permeability of the α phase, $\alpha = w, o, g$, respectively, and R_{so} be the gas

solubility. Then the mass conservation equations of the black oil model are [6–8]

$$-\nabla\cdot\left(\frac{\rho_{WS}}{B_w}u_w\right)+q_W=\frac{\partial}{\partial t}\left(\phi\frac{\rho_{WS}}{B_w}s_w\right)$$

for the water component,

$$-\nabla\cdot\left(\frac{\rho_{OS}}{B_o}u_o\right)+q_O=\frac{\partial}{\partial t}\left(\phi\frac{\rho_{OS}}{B_o}s_o\right)$$

for the oil component,

$$-\nabla\cdot\left(\frac{\rho_{GS}}{B_g}u_g+\frac{R_{\mathrm{so}}\rho_{GS}}{B_o}u_o\right)+q_G=\frac{\partial}{\partial t}\left[\phi\left(\frac{\rho_{GS}}{B_g}s_g+\frac{R_{\mathrm{so}}\rho_{GS}}{B_o}s_o\right)\right]$$

for the gas component, where $\rho_{\beta S}$ is the density of the β component at standard conditions (stock tank) and q_β is the mass flow rate of the β component at wells, $\beta=W,O,G$. The volumetric velocity of the α phase is represented by Darcy's law

$$u_\alpha=-\frac{KK_{r\alpha}}{\mu_\alpha}\nabla\Phi_\alpha,\quad \alpha=g,o,w$$

where the potential Φ_α of the α phase is given by

$$\Phi_\alpha=p_\alpha-\rho_\alpha\tilde{g}D,\quad \alpha=w,o,g$$

ρ_α represents the density of the α phase, $\tilde{g}$ is the gravitational constant, and D is the depth function. The saturations of the water, oil, and gas phases satisfy the constraint

$$s_w+s_o+s_g=1$$

Furthermore, the phase pressures are related by the capillary pressures p_{cow} and p_{cgo}:

$$p_{cow}=p_o-p_w,\quad p_{cgo}=p_g-p_o$$

Finally, the mass flow rates of wells are given by Peaceman's formulas [9]

$$q_O=\sum_{k=1}^{N_w}\sum_{m=1}^{M_{wk}}\frac{2\pi\Delta z_{k,m}}{\ln(r_{e,k}/r_{c,k})+s_{k,m}}\frac{KK_{ro}\rho_{OS}}{\mu_oB_o}[p_{bh,k}-p_o-\rho_o\tilde{g}(D_{w,k}-D)]\delta_{k,m}$$

$$q_W=\sum_{k=1}^{N_w}\sum_{m=1}^{M_{wk}}\frac{2\pi\Delta z_{k,m}}{\ln(r_{e,k}/r_{c,k})+s_{k,m}}\frac{KK_{rw}\rho_{WS}}{\mu_wB_w}[p_{bh,k}-p_w-\rho_w\tilde{g}(D_{w,k}-D)]\delta_{k,m}$$

$$q_G^g=\sum_{k=1}^{N_w}\sum_{m=1}^{M_{wk}}\frac{2\pi\Delta z_{k,m}}{\ln(r_{e,k}/r_{c,k})+s_{k,m}}\frac{KK_{rg}\rho_{GS}}{\mu_gB_g}[p_{bh,k}-p_g-\rho_g\tilde{g}(D_{w,k}-D)]\delta_{k,m}$$

$$q_G^o=\sum_{k=1}^{N_w}\sum_{m=1}^{M_{wk}}\frac{2\pi\Delta z_{k,m}}{\ln(r_{e,k}/r_{c,k})+s_{k,m}}\frac{KK_{ro}R_{\mathrm{so}}\rho_{GS}}{\mu_oB_o}[p_{bh,k}-p_o-\rho_o\tilde{g}(D_{w,k}-D)]\delta_{k,m}$$

where $\delta_{k,m}=\delta(x-x_{k,m})$ (the Dirac delta function at $x_{k,m}$), N_w is the total number of wells, $M_{w,k}$ is the total number of perforated zones of the kth well, $s_{k,m}$, $\Delta z_{k,m}$, and $x_{k,m}$ are the

skin factor, segment length, and central location of the mth perforated zone of the kth well, $r_{c,k}$ denotes the wellbore radius of the kth well, $r_{e,k}$ is the drainage radius of the kth well at the grid block in which $x_{k,m}$ is located, $p_{bh,k}$ is the bottom hole pressure of the kth well at datum $D_{w,k}$, and $q_G = q_G^g + q_G^o$.

The model is completed by specifying boundary and initial conditions. In this paper, we consider no flow boundary conditions

$$u_\alpha \cdot n = 0, \quad \alpha = w, o, g, \ \ x \in \partial\Omega$$

where n is the outward unit norm to the boundary $\partial\Omega$ of the reservoir domain Ω. The initial conditions depend on the state of a reservoir. When all gas dissolves into the oil phase, there is no gas phase present, i.e. $s_g = 0$. In such a case, the reservoir is called at the undersaturated state. If all three phases co-exist, the reservoir is referred to as at the saturated state. At the undersaturated state, we use $p = p_o$, s_w, and p_b as the unknowns [8], where p_b is the bubble point pressure. The corresponding initial conditions are

$$p(x,0) = p^0(x), \quad p_b(x,0) = p_b^0(x), \quad s_w(x,0) = s_w^0(x), \ \ x \in \Omega$$

At the saturated state, we employ $p = p_o$, s_w, and s_o as the unknowns. In this case, the initial conditions become

$$p(x,0) = p^0(x), \quad s_w(x,0) = s_w^0(x), \quad s_o(x,0) = s_o^0(x), \ \ x \in \Omega$$

5. APPLICATION OF THE GMRES TO SMU02

The simulator SMU02 is a general multicomponent, multiphase reservoir simulator based on the black oil model. It includes rectangular, PEBI, and Voronoi gridding techniques and finite difference, control volume finite element, and control volume function approximation discretization methods [10]. It consists of two major parts: the initialization SMU02I and the main body SMU02R. In the SMU02I, data such as fluid, rock, injection, production, grid, and control data are read from initial files, and then necessary data preparations are done for the SMU02R.

The SMU02R includes some major components like time and space discretization of the governing equations, Newton–Raphson linearizations, construction of Jacobian matrices, and solution of linear systems. The solution of linear systems is within each Newton–Raphson iteration. As noted, for a petroleum reservoir simulation with a number of gridblocks of order 100 000, about 80–90% of the total simulation time is spent on the system solution. In the original SMU02R, the linear solver is the ORTHOMIN(K), and the preconditioner M is based on ILU(K). In this paper, we discuss the application of the GMRES(m) to the SMU02R, and compare these two solvers. For a fair comparison, we use ILU(K) as the preconditioners for both of them. Other preconditioners are possible, such as those based on ILUT (a dual threshold incomplete LU factorization) and AMG (algebraic multigrid), which is being investigated and will be reported elsewhere.

6. NUMERICAL EXPERIMENTS

We carry out numerical experiments on a shared-memory machine, SGI Origin 2000 with eight 250 MHz processors and 4 G memory; each processor has 32 KB L1 cache for instructions, 32 KB L1 cache for data, and 4 MB L2 cache [11]. The convergent criterion for both the ORTHOMIN and GMRES is $\|r_k\|_2/\|RHS\|_2 \leqslant 10^{-4}$. In the subsequent tables TT and ST indicate the total and solver CPU times in seconds, respectively, and BMI is the number of iterations beyond the maximum number 100. The space discretization method used for all five models below is based on a block-centred finite difference method with harmonically averaged coefficients (equivalently, a mixed finite element method). The solution scheme is based on the fully implicit solution method; i.e. all the coupled equations are solved simultaneously. The number of restarts is ten, and the ILU(0) is used as the preconditioner for both the ORTHOMIN and GMRES.

6.1. Numerical model I

This simulation problem is chosen from the second case of the benchmark problem of the first CSP [12]. A grid of rectangular parallelepipeds for the reservoir under consideration is given in Figure 1, where the number of subintervals in the x-, y-, and z-direction is 10, 10, and 3, respectively. The diagonal cross-sectional view of this reservoir can be also seen in this figure. We briefly state the data; for more details on these data, see Reference [12].

At the initial state, the reservoir reaches equilibrium with initial reservoir pressure 4800 psia at 8400 ft and with reservoir temperature 200°F. The depth to the top of this reservoir is 8325 ft. The gas/oil (GOC) and water/oil contacts (WOC), respectively, are located at 8320 and 8450 ft. The capillary pressure is zero. The reservoir porosity measured at a pressure of 14.7 psia is 0.3. The rock compressibility is 3×10^{-6} 1/psi. The PVT function data for oil,

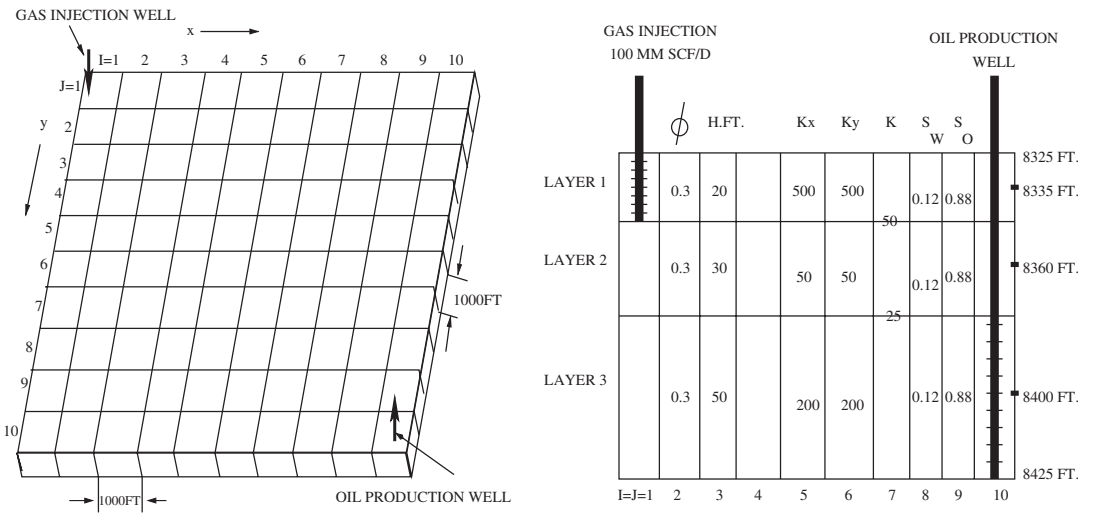

Figure 1. Left: reservoir and grid system; right: diagonal cross section.

Table I. Saturated oil PVT function data.

Pressure (psia)	FVF (RB/STB)	Viscosity (cp)	Density (lbm/cu ft)	Solution GOR (SCF/STB)
14.7	1.0620	1.0400	46.244	1.0
264.7	1.1500	0.9750	43.544	90.5
514.7	1.2070	0.9100	42.287	180.0
1014.7	1.2950	0.8300	41.004	371.0
2014.7	1.4350	0.6950	38.995	636.0
2514.7	1.5000	0.6410	38.304	775.0
3014.7	1.5650	0.5940	37.781	930.0
4014.7	1.6950	0.5100	37.046	1270.0
5014.7	1.8270	0.4490	36.424	1618.0
9014.7	2.3570	0.2030	36.482	2984.0

Table II. Saturated water PVT function data.

Pressure (psia)	FVF (RB/STB)	Viscosity (cp)	Density (lbm/cu ft)	Gas/water ratio (SCF/STB)
14.7	1.0410	0.3100	62.238	0.0
264.7	1.0403	0.3100	62.283	0.0
514.7	1.0395	0.3100	62.328	0.0
1014.7	1.0380	0.3100	62.418	0.0
2014.7	1.0350	0.3100	62.599	0.0
2514.7	1.0335	0.3100	62.690	0.0
3014.7	1.0320	0.3100	62.781	0.0
4014.7	1.0290	0.3100	62.964	0.0
5014.7	1.0258	0.3100	63.160	0.0
9014.7	1.0130	0.3100	63.959	0.0

water, and gas are, respectively, given in Tables I–V, where FVF stands for the formation volume factor. The horizontal and vertical absolute permeability distribution and the initial water and oil saturation distribution are indicated in Figure 1. The saturation function data are listed in Table VI.

There are a gas injection well and an oil production well, whose wellbore radii are 0.25 ft. Their locations are shown in Figure 1. They completely perforate at the first and third zone, respectively. The gas injection rate is 100 MMSCF/D. The maximum and minimum oil production rates of the production well are, respectively, 20 000 STB/D and 1000 STB/D, and the minimum flowing bottom hole pressure is 1000 psia. The run of the simulator is terminated at the end of the 10th year. The CPU times for the ORTHOMIN and GMRES are displayed in Table VII. From this table we do not see much speed-up of the GMRES for this small simulation problem.

6.2. Numerical model II

This model problem is the same as the previous one. We just refine the grid in the x- and y-directions. Now, the number of subintervals in these two directions is 70, and the total

Table III. Gas PVT function data.

Pressure (psia)	FVF (RB/STB)	Viscosity (cp)	Density (lbm/cu ft)	Pseudo gas potential (psia/cp)
14.7	0.166666	0.008000	0.0647	0.0
264.7	0.012093	0.009600	0.8916	0.777916 E+07
514.7	0.006274	0.011200	1.7185	0.267580 E+08
1014.7	0.003197	0.014000	3.3727	0.875262 E+08
2014.7	0.001614	0.018900	6.6806	0.270709 E+09
2514.7	0.001294	0.020800	8.3326	0.386910 E+09
3014.7	0.001080	0.022800	9.9837	0.516118 E+09
4014.7	0.000811	0.026800	13.2952	0.803963 E+09
5014.7	0.000649	0.030900	16.6139	0.112256 E+10
9014.7	0.000386	0.047000	27.9483	0.251845 E+10

Table IV. Undersaturated oil PVT function data.

Pressure (psia)	FVF (RB/STB)	Viscosity (cp)	Density (lbm/cu ft)
4014.7	1.6950	0.5100	37.046
9014.7	1.5790	0.7400	39.768

Table V. Undersaturated water PVT function data.

Pressure (psia)	FVF (RB/STB)	Viscosity (cp)	Density (lbm/cu ft)
4014.7	1.0290	0.3100	62.964
9014.7	1.0130	0.3100	63.959

number of grid points is 14 700. For such a simulation problem with small grid blocks and with a long simulation time (10 years), stability of the numerical solution to the problem is very important. Both the ORTHOMIN and GMRES work very well for this problem, and their CPU times are given in Table VIII. We see that the GMRES uses only 63.78% of the CPU time of the ORTHOMIN when the grid in model I is refined.

6.3. Numerical model III

This is the benchmark problem of the second SPE CSP for three-phase coning flow [13]. The physical data are briefly reviewed; for more details, see Reference [13]. The reservoir and a cross-sectional view is seen in Figure 2. The reservoir dimensions, permeabilities, and porosities are presented in Table IX, where K_h and K_v denote the horizontal and vertical permeabilities, respectively. The radial extent of the reservoir is 2050 ft. In the radial direction, 10 blocks are used. Their boundaries are at 2.00, 4.32, 9.33, 20.17, 43.56, 94.11, 203.32, 439.24, 948.92, and 2050 ft, respectively. There are 15 vertical layers. The depth to the top of formation is 9000 ft. The pore, water, oil, undersaturated oil, and oil viscosity compressibilities are

Table VI. Relative permeability data of model I.

s_g	K_{rg}	K_{ro}
0.0	0.0	1.0
0.001	0.0	1.0
0.02	0.0	0.997
0.05	0.005	0.980
0.12	0.025	0.700
0.2	0.075	0.350
0.25	0.125	0.200
0.30	0.190	0.090
0.40	0.410	0.021
0.45	0.60	0.010
0.50	0.72	0.001
0.60	0.87	0.0001
0.70	0.94	0.000
0.85	0.98	0.000
1.0	1.0	0.000

Table VII. CPU times of the ORTHOMIN and GMRES for model I.

Method	TT(s)	ST(s)	Days	BMI
ORTHOMIN	40.24	37.17	3650.0	0
GMRES	29.75	26.50	3650.0	0

Table VIII. CPU times of the ORTHOMIN and GMRES for model II.

Method	TT(s)	ST(s)	Days	BMI
ORTHOMIN	24 188.76	22 799.07	3650.0	319
GMRES	16 074.37	14 541.31	3650.0	268

4×10^{-6}, 4×10^{-6}, 3×10^{-6}, and 0 psi^{-1}, respectively. The stock-tank densities for oil and water are 45.0 and 63.02 lbm/cu ft. The gas density at the standard condition is 0.0702 lbm/cu ft. The depths to the GOC and WOC are 9035 and 9209 ft, respectively. The reservoir is initially at capillary/gravity equilibrium with a pressure of 3600 psia at the GOC. The capillary pressures at the GOC and WOC are zero. The single well at the centre of the radial system completely perforates at the 7th and 8th layers, has the wellbore radius 0.25 ft, and has a minimum bottom hole pressure of 3000 psia. The saturation function data and PVT property data are presented in Tables X–XII and the well production schedule is shown in Table XIII.

The finite difference method in the (r,z)-co-ordinate system is used for the space discretization. The total number of grid blocks is 10×15, and the final time of simulation is 900 days. The CPU times for the ORTHOMIN and GMRES are given in Table XIV. Again, for this small problem we do not see much advantage of the GMRES over the ORTHOMIN. When the grid is refined, we have observed a similar speed-up as in the previous model.

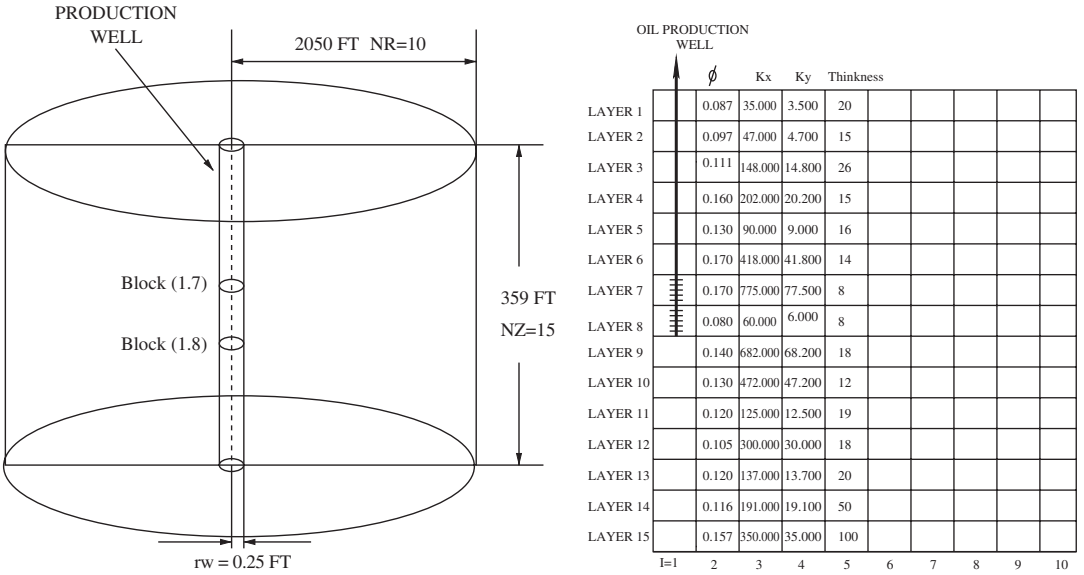

Figure 2. Left: simulation domain; right: a cross section.

Table IX. Reservoir description of model III.

Layer	Thickness (ft)	K_h (md)	K_v (md)	Porosity
1	20	35.000	3.500	0.087
2	15	47.500	4.750	0.097
3	26	148.000	14.800	0.111
4	15	202.000	20.200	0.160
5	16	90.000	9.000	0.130
6	14	418.500	41.850	0.170
7	8	775.000	77.500	0.170
8	8	60.000	6.000	0.080
9	18	682.000	68.200	0.140
10	12	472.000	47.200	0.130
11	19	125.000	12.500	0.120
12	18	300.000	30.000	0.105
13	20	137.000	13.750	0.120
14	50	191.000	19.100	0.116
15	100	350.000	35.000	0.157

6.4. Numerical model IV

This simulation model comes from a development scheme design for water flooding of a real oil field. The dimensions of this oil field are 6890 ft $\times$ 6726 ft $\times$ 4227 ft. It has four geological layers with an irregularly shaped boundary, top, and base and with reservoir temperature 165.2°F. The absolute permeability and compressibility of rock and the thickness of the

Table X. Saturation function data of model III for water/oil.

s_w	K_{rw}	K_{row}	p_{cow} (psi)
0.22	0.0	1.0	7.0
0.30	0.07	0.4000	4.0
0.40	0.15	0.1250	3.0
0.50	0.24	0.0649	2.5
0.60	0.33	0.0048	2.0
0.80	0.65	0.0	1.0
0.90	0.83	0.0	0.5
1.00	1.0	0.0	0.0

Table XI. Saturation function data of model III for gas/oil.

s_g	K_{rg}	K_{rog}	p_{cgo} (psi)
0.0	0.0	1.0	0.0
0.04	0.0	0.60	0.2
0.10	0.0220	0.33	0.5
0.20	0.1000	0.10	1.0
0.30	0.2400	0.02	1.5
0.40	0.3400	0.0	2.0
0.50	0.4200	0.0	2.5
0.60	0.5000	0.0	3.0
0.70	0.8125	0.0	3.5
0.78	1.0	0.0	3.9

Table XII. PVT property data of model III.

P (psia)	B_o (RB/STB)	μ_o (cp)	R_{so} (SCF/STB)	B_w (RB/STB)	μ_w (cp)	B_g (RB/STB)	μ_g (cp)
400	1.0120	1.17	165	1.01303	0.96	5.90	0.0130
800	1.0255	1.14	335	1.01182	0.96	2.95	0.0135
1200	1.0380	1.11	500	1.01061	0.96	1.96	0.0140
1600	1.0150	1.08	665	1.00940	0.96	1.47	0.0145
2000	1.0630	1.06	828	1.00820	0.96	1.18	0.0150
2400	1.0750	1.03	985	1.00700	0.96	0.98	0.0155
2800	1.0870	1.00	1130	1.00580	0.96	0.84	0.0160
3200	1.0985	0.98	1270	1.00460	0.96	0.74	0.0165
3600	1.1100	0.95	1390	1.00341	0.96	0.65	0.0170
4000	1.1200	0.94	1500	1.00222	0.96	0.59	0.0175
4400	1.1300	0.92	1600	1.00103	0.96	0.54	0.0180
4800	1.1400	0.91	1676	0.99985	0.96	0.49	0.0185
5200	1.1480	0.90	1750	0.99866	0.96	0.45	0.0190
5600	1.1550	0.89	1810	0.99749	0.96	0.42	0.0195

layers are variant in space. The water, oil, and oil viscosity compressibilities are 3.1×10^{-6}, 3.1×10^{-6}, and 0 psi^{-1}, respectively. The stock-tank densities for oil and water are, respectively, 60.68 and 62.43 lbm/cu ft. The gas specific gravity at the standard condition (expressed

Table XIII. Production schedule.

Period number	Time period (day)	Oil production rate (STB/D)
1	1–10	1000
2	10–50	100
3	50–720	1000
4	720–900	100

Table XIV. CPU times of the ORTHOMIN and GMRES for model III.

Method	TT(s)	ST(s)	Days	BMI
ORTHOMIN	7.60	6.09	900.0	0
GMRES	7.54	5.76	900.0	0

Table XV. PVT property data of model IV.

P (psia)	B_o (RB/STB)	μ_o (cp)	R_{so} (SCF/STB)	B_w (RB/STB)	μ_w (cp)	Z_g	μ_g (cp)
87.02	1.0057	52.8	6.74	1.022	0.42	0.993	0.0151
435.11	1.0208	37.6	9.19	1.022	0.42	0.966	0.0141
870.23	1.0415	26.3	83.66	1.022	0.42	0.936	0.0132
1305.34	1.0632	19.7	130.25	1.022	0.42	0.913	0.0141
1624.42	1.0795	15.5	165.63	1.022	0.42	0.898	0.0151

as the ratio of the molecular weight of the gas to the molecular weight of air) is 0.5615. The depths to the GOC and WOC are 3666 and 4593 ft, respectively. The reservoir is initially at capillary/gravity equilibrium with a pressure of 1624 psia at depth 3684 ft. The capillary pressures at the GOC and WOC are zero. Other PVT and rock data are given in Tables XV–XVII, where Z_g is the gas deviation factor.

There are 50 oil production wells and 20 water injection wells. They perforate all the layers (above the WOC). The wellbore radius of each well is 0.25 ft. The well controls can be the bottom hole pressure, water injection rate, oil production rate, and liquid production rate controls with a water cut limit of 0.95. The number of subintervals in the x-, y-, and z-direction is 42, 41, and 4, respectively (there are 6888 grid blocks). The CPU times for the ORTHOMIN and GMRES at 6000 days are presented in Table XVIII. For this simulation problem of a moderate size, we see that the GMRES is superior to the ORTHOMIN, and uses only 80.27% of the CPU time of the ORTHOMIN.

6.5. Numerical model V

Finally, we compare the ORTHOMIN and GMRES for another large, real oil reservoir in South America to simulate the behaviour of a water flooding process and to predict the

Table XVI. Saturation function data of model IV for water/oil.

s_w	K_{rw}	K_{row}	p_{cow} (psi)
0.2400	0.000	1.000	2.4656
0.3050	0.001	0.809	1.1603
0.3266	0.002	0.707	0.8702
0.3483	0.004	0.606	0.5802
0.3699	0.007	0.513	0.3916
0.3915	0.010	0.421	0.2321
0.4131	0.014	0.349	0.1450
0.5000	0.037	0.260	0.0725
0.6000	0.087	0.200	0.0435
0.7000	0.155	0.150	0.0232
0.8000	0.230	0.100	0.0000
0.9000	0.400	0.000	0.0000
1.0000	1.000	0.000	0.0000

Table XVII. Saturation function data of model IV for gas/oil.

s_g	K_{rg}	K_{rog}	p_{cgo} (psi)
0.00	0.000	1.0000	0.0
0.04	0.000	0.4910	0.0
0.10	0.001	0.2990	0.0
0.20	0.003	0.1200	0.0
0.22	0.007	0.1030	0.0
0.29	0.015	0.0400	0.0
0.33	0.030	0.0210	0.0
0.37	0.065	0.0087	0.0
0.40	0.131	0.0021	0.0
0.46	0.250	0.0000	0.0
0.76	1.000	0.0000	0.0

Table XVIII. CPU times of the ORTHOMIN and GMRES for model IV.

Method	TT(s)	ST(s)	Days	BMI
ORTHOMIN	1804.48	1693.91	6000.0	53
GMRES	1480.33	1359.69	6000.0	55

performance of this reservoir. The outline of this reservoir is as follows:

- The reservoir is undersaturated. The initial formation pressure equals 11 800 psia and the initial bubble point pressure is 3157 psia.
- The datum depth is 15 500 ft and the depth of WOC is 17 200 ft.
- The surface oil density is 57.06 lbm/ft^3, the oil formation factor is 1.446, the oil viscosity in the reservoir is 0.679 cp, and the oil–water viscosity ratio is 3.3.
- The geological features are: 40 sandstone layers; the 11th and 30th layers—sealing; three independent development units divided in the vertical direction; the western and eastern regions divided by a fault in the reservoir.

Table XIX. CPU times of the ORTHOMIN and GMRES for model V.

Method	TT(s)	ST(s)	Days	BMI
ORTHOMIN	65,851.49	61,768.02	4901.0	786
GMRES	42,948.90	38,734.54	4901.0	488

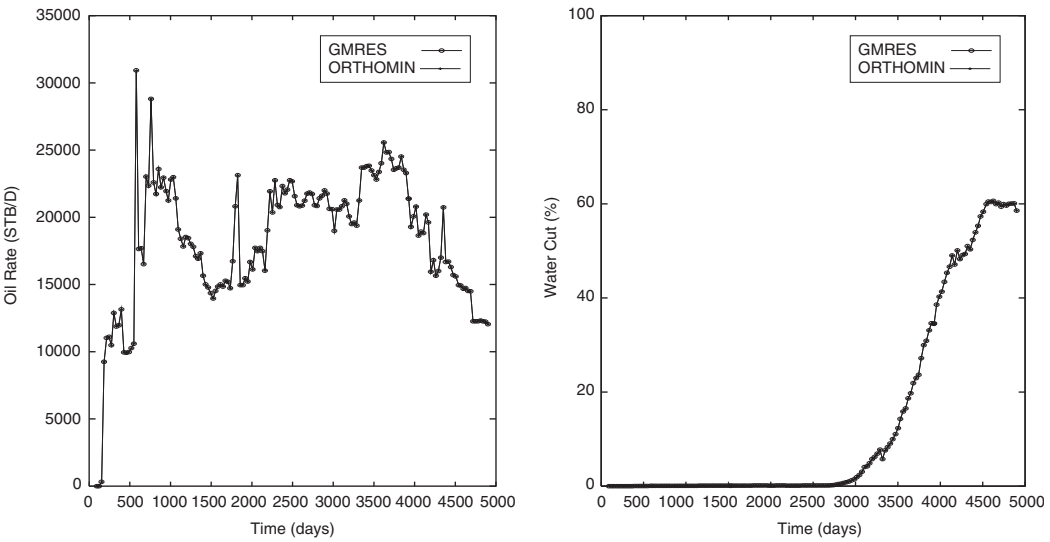

Figure 3. Left: oil production rate; right: water cut.

- The reservoir has been developed for 13.5 years: 5.3 years—natural reservoir drive; 8.2 years—water injection.
- 24 wells have been drilled. 10 oil production wells and 5 water injection wells are used to develop this reservoir in the current period.

The dimensions of the partition of the simulation domain Ω are $63 \times 31 \times 40$, and the CPU times at 4901 days are given in Table XIX. For this model problem, we see that the GMRES uses as much as 63% of the CPU time of the ORTHOMIN. As an illustration, the daily oil production rate, water cut (the ratio of the water production rate to the sum of the water and oil production rates), average reservoir pressure, and oil recovery curves obtained using both solvers are presented in Figures 3 and 4. The curves from these two solvers match perfectly.

7. CONCLUDING REMARKS

We have compared the ORTHOMIN and GMRES for five numerical models. For a fixed model, we also consider the relative efficiency defined by $1 - t_{\mathrm{GMRES}}/t_{\mathrm{ORTHOMIN}}$, where t_{GMRES}

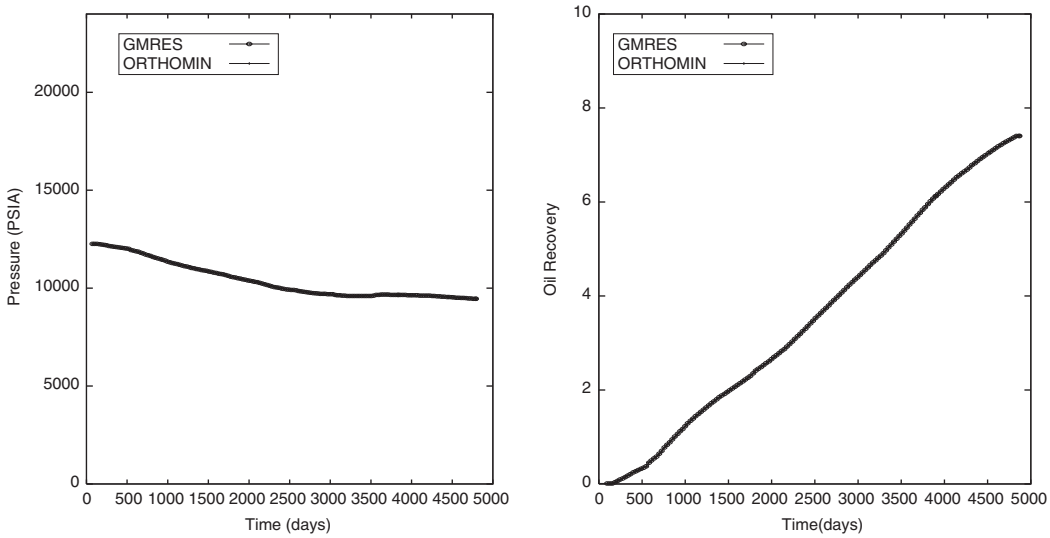

Figure 4. Left: average reservoir pressure; right: oil recovery.

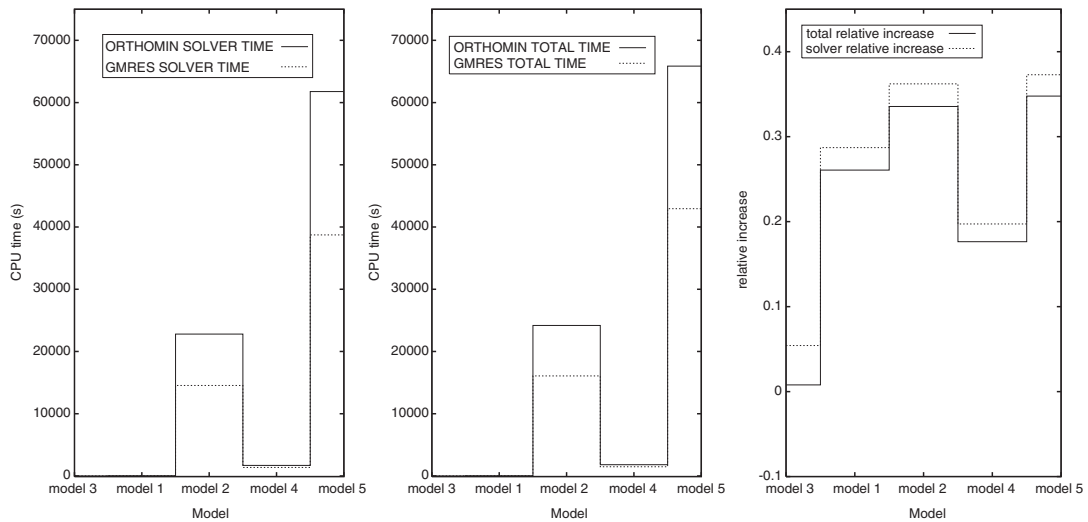

Figure 5. Comparison of the ORTHOMIN and GMRES for all models.

and t_{ORTHOMIN} are the CPU times of these two algorithms, respectively. The comparisons between these two algorithms in terms of the CPU time and relative efficiency for all models and the CPU time vs the simulation time for models IV and V are listed in Figures 5 and 6, respectively.

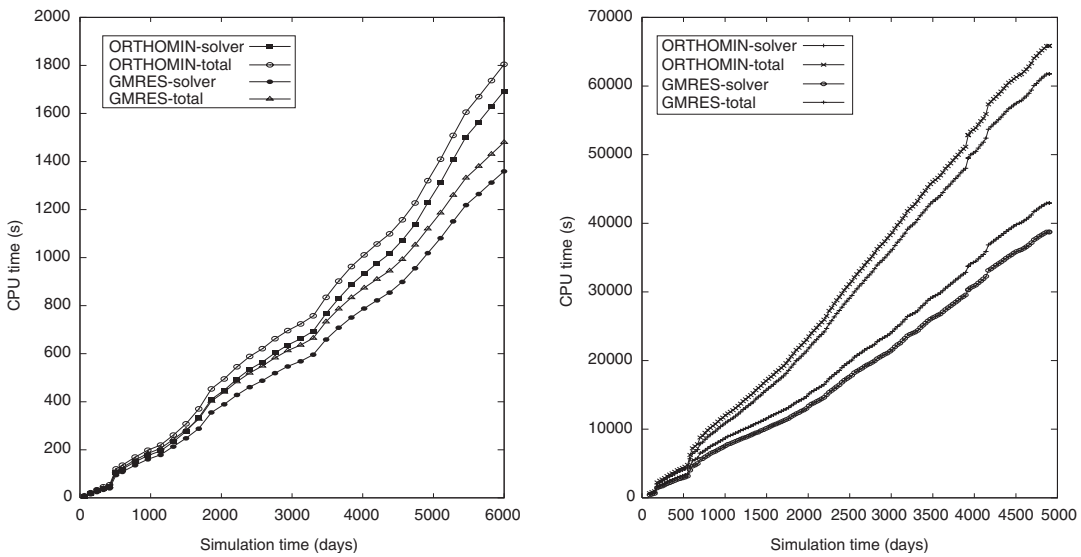

Figure 6. Comparison of the CPU vs simulation times for models IV and V.

From these figures, we can make the following remarks:

- The GMRES is faster than the ORTHOMIN for all five models tested.
- Model II is a refinement of model I; their partition dimensions are, respectively, $70 \times 70 \times 3$ and $10 \times 10 \times 3$. For these two models, the relative efficiency is 0.3622 and 0.2871 for the solution time and 0.3355 and 0.2607 for the total simulation time, respectively. The GMRES efficiency increases with the size of matrices.
- Models IV and V are complex, real oil field problems. Model IV has 70 wells and 6888 gird blocks, where 4608 of them are active, and its final simulation time is 6000 days. Model V has 24 wells and 79 360 grid blocks, where 28 579 of them are active, and its final simulation time is 4901 days. The comparisons for these two models in terms of the CPU time vs the simulation time are given in Figure 6. For these two models, the relative efficiency is 0.1973 and 0.3729 for the solution time and 0.1796 and 0.3478 for the total simulation time, respectively. Again, the GMRES efficiency increases with the size of matrices and the length of simulation time.

In this paper, we have used the finite difference method for discretization of the governing equations of the black oil model on structured grids. We are investigating the application of the control volume finite element method to this model on unstructured grids and of the ORTHOMIN and GMRES to the resulting systems of algebraic equations. The comparison between these two solvers on the unstructured grids will be done in future study.

REFERENCES

1. Vinsome PKW. ORTHOMIN, an iterative method for solving sparse sets of simultaneous linear equations. *Proceedings of the Fourth Symposium on Reservoir Simulations*, Society of Petroleum Engineers of AIME, 1976; 149–157.

2. Saad Y, Schultz MH. GMRES: a generalized minimal residual algorithm for solving nonsymmetric linear systems. *SIAM Journal on Science*, *Statistics and Computation* 1986; **7**:856–869.
3. Choquet R, Erhel J. Newton-GMRES algorithm applied to compressible flows. *International Journal for Numerical Methods in Fluids* 1996; **23**:177–190.
4. Saad Y. A flexible inner–outer preconditioned GMRES algorithm. *SIAM Journal on Science*, *Statistics and Computation* 1993; **14**:461–469.
5. Golub GH, van Loan CF. *Matrix Computations*. Johns Hopkins University Press: Baltimore, London, 1983.
6. Bear J. *Dynamics of Fluids in Porous Media*. Dover: New York, 1972.
7. Chen Z. Formulations and numerical methods for the black-oil model in porous media. *SIAM Journal on Numerical Analysis* 2000; **38**:489–514.
8. Li B, Chen Z, Huan G. Control volume function approximation methods and their applications to modeling porous media flow II: the black oil model. *Advances in Water Resources* 2004; **27**:99–120.
9. Peaceman DW. Interpretation of well-block pressures in numerical reservoir simulation. *SPE 6893*, *52nd Annual Fall Technical Conference and Exhibition*, Denver, 1977.
10. Chen Z, Li B, Huan G, Espin D, Klie H, Buitrago S. Control volume function approximation method for the black oil model. *Proceedings of the 2nd Meeting on Reservoir Simulation*, Universidad Argentina de la Empresa, Buenos Aires, Argentina, 5–6 November 2002, CD-ROM.
11. SGI, Origin 2000 and Onyx2 performance tuning and optimization guide. *SGI Document Number 007-3430-003*.
12. Odeh AS. Comparison of solutions to a three-dimensional black-oil reservoir simulation problem. *Journal of Petroleum Technology* 1981; **January**:13–25.
13. Weinstein HG, Chappelear JE, Nolen JS. Second comparative solution project: a three-phase coning study. *Journal of Petroleum Technology* 1986; **March**:345–354.

